J|A|C|S ARTICLES

Published on Web 08/13/2010

Self-Assembled Inverted Micelles Stabilize Ionic Liquid Domains in Supercritical CO_2

Aneesh Chandran, Karthigeyan Prakash, and Sanjib Senapati*

Department of Biotechnology, Indian Institute of Technology Madras, Chennai 600036, India,

Received July 7, 2010; E-mail: sanjibs@iitm.ac.in

Abstract: Molecular aggregation is a complex phenomenon that is difficult to study in detail experimentally. Here, we elucidate the formation of ionic liquid-in-carbon dioxide (IL-in-CO_2) microemulsions *via* a computer simulation technique that demonstrates the entire process of self-aggregation at the atomic level. Our study reveals direct evidence of the existence of stable IL droplets within a continuous CO_2 phase through amphiphilic surfactants. The microstructure of the nanodroplets matches very well with the small-angle neutron scattering data. A detailed investigation of the structural and energetic properties explains why guanidium acetate-based IL-in-CO_2 microemulsions showed a greater stability than imidazolium hexafluorophosphate-based microemulsions in recent spectroscopic experiments. In contrast to the existing hypothesis in literature, the study reveals that the stability of the microemulsions mainly pertains to the IL anion−headgroup interactions, while the cations play a secondary role. The detailed atomic level understanding provides a deeper insight that could help in designing new surfactants for improved IL uptake in CO_2.

1. Introduction

Room temperature ionic liquids (ILs) are organic salts, composed of organic cations and organic or inorganic anions, and are liquid at room temperature. Due to their unique properties, such as chemical stability, nonflammability, and low volatility, ILs are regarded as green solvents.[1−3] This in conjunction with their ease of preparation at different cation−anion combinations provides a great opportunity to obtain task-specific ILs for a range of applications, such as separations, synthesis, and catalytic reactions.[4−6]

Carbon dioxide in the supercritical state ($scCO_2$) has been identified as another environmentally benign solvent because it is nontoxic, nonflammable, and potentially recyclable. The potential of this abundant and easily tunable solvent is therefore being exploited on a variety of fronts, including extraction of caffeine from coffee, homogeneous and heterogeneous polymerization, synthesis of nanoparticles, and materials processing.[7−10] However, CO_2 is a low dielectric constant fluid, and many important classes of polar substances, including ILs exhibit low solubility in $scCO_2$.[11,12]

One of the major targets of modern chemistry is to combine the advantages of both these green solvents by improving the IL solubility in $scCO_2$. An effective way is to create microemulsions, containing IL droplets in continuous CO_2 phase, with the help of amphiphilic surfactants.[13] The polar IL molecules are comfortable being shielded by surfactant heads as much as possible, whereas the nonpolar CO_2 molecules are comfortable in direct interaction with surfactant tails. The significance is that the surfactant assemblies provide hydrophilic nanodomains in lipophilic phase, which finds potential uses as media for reactions between polar and nonpolar molecules, extraction of hydrophiles etc. Unfortunately, only a handful of studies on IL-in-CO_2 systems have been carried out, although the analogous water-in-CO_2 microemulsion systems were explored and extended to various applications during the past decade. Thus, Johnston and co-workers[12,14] had created a bulk water domain in continuous CO_2 phase using a commercially available perfluoropolyether surfactant, which could successfully extract hydrophiles including proteins. Chaitanya and Senapati[15] had shown that the extracted proteins in water-in-CO_2 microemulsions retain

(1) Rogers, R. D.; Seddon, K. R. *Science* **2003**, *302*, 792–793. Gorman, J. *Sci. News* **2001**, *160*, 156–158.
(2) Wasserscheid, P.; Keim, W. *Angew. Chem.* **2000**, *112*, 3926–3945.
(3) Welton, T. *Chem. Rev.* **1999**, *99*, 2071–2084.
(4) Wu, W.; Han, B.; Gao, H.; Liu, Z.; Jiang, T.; Huang, J. *Angew. Chem., Int. Ed.* **2004**, *43*, 2415–2417. Bates, E. D.; Mayton, R. D.; Ntai, I.; Davis, J. H., Jr. *J. Am. Chem. Soc.* **2002**, *124*, 926–927.
(5) Cooper, E. R.; Andrews, C. D.; Wheatley, P. S.; Webb, P. B.; Wormald, P.; Morris, R. E. *Nature* **2004**, *430*, 1012–1016. Li, Z.; Liu, Z.; Zhang, J.; Han, B.; Du, J.; Gao, Y.; Jiang, T. *J. Phys. Chem. B* **2005**, *109*, 14445–14448.
(6) Cole-Hamilton, D. J. *Science* **2003**, *299*, 1702–1706. Bluhm, M. E.; Bardley, M. G.; Butterick, R., III; Kusari, U.; Sneddon, L. G. *J. Am. Chem. Soc.* **2006**, *128*, 7748–7749.
(7) Adam, D. *Nature* **2000**, *407*, 938–940. Leitner, W. *Acc. Chem. Res.* **2002**, *35*, 746–756.
(8) Shah, P. S.; Holmes, J. D.; Doty, R. C.; Johnston, K. P.; Korgel, B. *J. Am. Chem. Soc.* **2000**, *122*, 4245–4246.
(9) Cooper, A. I. *Adv. Mater.* **2001**, *13*, 1111–1114.
(10) Adamsky, F. A.; Beckman, E. J. *Macromolecules* **1994**, *27*, 312–314.
(11) Blanchard, L. A.; Hancu, D.; Bechman, E. J.; Brennecke, J. F. *Nature* **1999**, *399*, 28–29.
(12) Johnston, K. P.; Harrison, K. L.; Clarke, M. J.; Howdle, S. M.; Heitz, M. P.; Bright, F. V.; Carlier, C.; Randolph, T. W. *Science* **1996**, *271*, 624–626.
(13) Liu, J.; Cheng, S.; Zhang, J.; Feng, X.; Fu, X.; Han, B. *Angew. Chem., Int. Ed.* **2007**, *46*, 3313–3315.
(14) Nagashima, K.; Lee, C. T.; Xu, B.; Johnston, K. P.; DeSimone, J. M.; Johnson, C. S., Jr. *J. Phys. Chem. B* **2003**, *107*, 1962–1968.
(15) Chaitanya, V. S. V.; Senapati, S. *J. Am. Chem. Soc.* **2008**, *130*, 1866–1870.

their native state. DeSimone and co-workers[16,17] had designed a variety of surfactants which provided an extended stability to the aqueous phase in CO_2, thereby expanding potential applications of the green $scCO_2$. A number of molecular dynamics (MD) simulation studies were also reported by various groups that provide structural details of this delicate interface.[18−20] The literature is, however, scanty for IL-based microemulsions. Eastoe et al.[21] carried out small-angle neutron scattering (SANS) experiments on IL-in-oil microemulsions which successfully detected the nanometer-sized dispersed IL droplets in oil. In a recent report, Han and co-workers[13] had shown the existence of IL domains in continuous CO_2 phase from their spectroscopic experiments on the mixtures of 1,1,3,3-tetramethylguanidium acetate ($[(CH_3)_2N]_2C{=}NH_2{}^+CH_3COO^-$; [TMG][Ac]), supercritical CO_2, and *N*-ethyl perfluorooctyl sulfonamide ($C_2H_5NHSO_2C_8F_{17}$; N-EtFOSA) surfactants. From the absorbed wavelength of the added probes, they concluded that the IL droplets were entrapped in reverse micellar cavities. Though this study provides (indirect) evidence of the formation of IL-in-CO_2 microemulsions, the structural characteristics of the droplets and the basis of their stability were not clear.

Here, we provide the direct evidence of the formation of nanometer-sized, ellipsoidal-shaped IL domains in bulk CO_2 by carrying out detailed molecular dynamics simulations of the mixtures of [TMG][Ac]/N-EtFOSA/CO_2 and a range of other related IL-in-CO_2 systems. To avoid any dependency on initial conditions, we started our simulations from a completely random configuration, and for a higher accuracy, we carried out all-atom, unrestrained MD simulations. The simulation results demonstrate the entire process of self-aggregation, where the polar components settle together in the apolar media through the amphiphilic interface. The atomic-level interaction profiles explain why [TMG][Ac]-based IL-in-CO_2 microemulsions showed greater stability than 1-butyl-3-methylimidazolium hexafluorophosphate ([BMIM][PF_6])-based microemulsions in recent spectroscopic experiments.[13] The exploration of a variety of other ILs reveals that the stability of the microemulsions mainly pertains to the IL anion−headgroup interactions, while the cations play a secondary role. In short, our study not only complements the experimental findings but also provides a wealth of detailed information at atomic level which is very difficult to achieve experimentally.

2. The Model and Simulation Details

We performed MD simulations on a series of random ternary mixtures, composed of IL, $scCO_2$, and N-EtFOSA surfactants. The ternary mixtures differ from each other in IL content. While the first mixture (system 1) contained [TMG][Ac] as the IL, the second mixture (system 2) contained [BMIM][PF_6] in place of [TMG][Ac]. Five additional systems were explored by varying the IL, as listed in Table 1. These systems were studied at IL-to-surfactant molar ratio, $W_o = 0.8$. System 1 was further examined at two different compositions, corresponding to $W_o = 0.4$ and 1.2. Thus, we have investigated seven different IL-in-CO_2 systems and performed a total of nine simulations in this work.

Table 1. Average Interaction Energy (E in kcal/mol), H-Bond Distance (d in Å), and the Probability of H-Bond Formation (P) between Anion and Headgroups (A−HG), Cation and Headgroups (C−HG) in Systems 1−7. Possible Mode of Interactions are, acetate−HG: $COO^-\cdots H{-}N$; TMG−HG: $NH_2{}^+\cdots O{=}S$; PF_6−HG: $PF^-\cdots H{-}N$; BMIM−HG: $C_RH^+\cdots O{=}S$; chloride−HG: $Cl^-\cdots H{-}N$; nitrate−HG: $NO^-\cdots H{-}N$; BF_4−HG: $BF^-\cdots H{-}N$

System	IL	E_{A-HG}	E_{C-HG}	$d^{H\text{-}bond}_{A-HG}$	$d^{H\text{-}bond}_{C-HG}$	P_{A-HG}	P_{C-HG}
1	[TMG][Ac]	−5.62	−3.21	1.91	2.15	0.99	0.15
2	[BMIM][PF_6]	−2.01	−1.17	2.13	2.38	0.96	0.29
3	[TMG][PF_6]	−2.42	−2.37	2.09	2.16	0.96	0.12
4	[BMIM][Ac]	−5.27	−1.36	1.85	2.38	0.99	0.34
5	[BMIM][Cl]	−6.12	−2.12	2.24	2.39	1.00	0.31
6	[BMIM][NO_3]	−4.12	−1.14	1.84	2.37	0.99	0.29
7	[BMIM][BF_4]	−2.51	−1.01	2.11	2.35	0.97	0.27

The interaction potentials for the ILs are obtained from the work of Padua[22] and Senapati[23] which are developed within the spirit of OPLS-AA/AMBER framework. The proposed parameters were shown to reproduce the experimental crystal structure and/or the liquid density data accurately. Table S1 in Supporting Information lists all the parameters adopted in this study. To model the N-EtFOSA surfactant, we have used the OPLS-AA potentials of sulfonamide and perfluoroalkanes developed by Jorgensen.[24] The missing dihedral parameters are derived here within the spirit of OPLS-AA/AMBER framework by using a model compound, $CH_3{-}CH_2{-}NH{-}SO_2{-}CF_2{-}CF_2{-}CF_2{-}CF_3$. Ab initio calculations with the 6-31+G* basis set, using the Gaussian 03 program,[25] yielded energy profiles for rotation about the unknown dihedrals, δ. For each optimized geometry corresponding to a particular value of δ, an energy minimization neglecting the contribution from the dihedral of interest was performed using the SANDER module of the Amber 9.0 program.[26] The difference in energy between *ab initio* and molecular mechanics (MM) calculations was fitted to obtain the dihedral parameters, as included in Table S1 (Supporting Information). Partial charges are obtained via fits to the electrostatic potential surfaces from *ab initio* molecular orbital calculations with the 6-31+G* basis set, such that the calculated electrostatic potential values surrounding N-EtFOSA were well reproduced by the obtained partial atomic charges. The derived force field is validated against the available experimental crystal structure data (Table S2, Supporting Information). The three-site EPM2 model,[27] proposed by Harris and Yung is used to describe the CO_2 molecules. This model accurately reproduces the experimental critical point and liquid−vapor coexistence curve and is being widely used. The

(16) Keiper, J. S.; Simhan, R.; DeSimone, J. M.; Wignall, G. D.; Melnichenko, Y. B.; Frielinghaus, H. *J. Am. Chem. Soc.* **2002**, *124*, 1834–1835.
(17) Cooper, A. I.; Londono, J. D.; Wignall, G.; McClain, J. B.; Samulski, E. T.; Lin, J. S.; Dobrynin, A.; Rubinstein, M.; Burke, A. L. C.; Frechet, J. M. J.; DeSimone, J. M. *Nature* **1997**, *389*, 368–371.
(18) Senapati, S.; Berkowitz, M. L. *J. Phys. Chem. B* **2003**, *107*, 12906–12916.
(19) Senapati, S.; Keiper, J. S.; DeSimone, J. M.; Wignall, G. D.; Melnichenko, Y. B.; Frielinghaus, H.; Berkowitz, M. L. *Langmuir* **2002**, *18*, 7371–7376.
(20) Salaniwal, S.; Cui, S. T.; Cochran, H. D.; Cummings, P. T. *Langmuir* **2001**, *17*, 1773–1783. Langmuir 2001, *17*, 1784−1792.
(21) Eastoe, J.; Gold, S.; Rogers, S. E.; Paul, A.; Welton, T.; Heenan, R. K.; Grillo, I. *J. Am. Chem. Soc.* **2005**, *127*, 7302–7303.
(22) Lopes, J. N. C.; Padua, A. A. H. *J. Phys. Chem. B* **2006**, *110*, 19586–19592. Lopes, J. N. C.; Deschamps, J.; Padua, A. A. H. *J. Phys. Chem. B* **2004**, *108*, 2038–2047. Lopes, J. N. C.; Padua, A. A. H. *J. Phys. Chem. B* **2004**, *108*, 16893–16898.
(23) Chandran, A.; Prakash, K.; Senapati, S. *Chem. Phys.* **2010**, DOI: 10.1016/j.chemphys.2010.06.011.
(24) Hertzog, D. K. J.; Jorgensen, W. L. *J. Med. Chem.* **1997**, *40*, 1539–1549. Watkins, E. K.; Jorgensen, W. L. *J. Phys. Chem. A* **2001**, *105*, 4118–4125.
(25) Frisch M. J.; et al. *Gaussian 03*, revision C.02; Gaussian Inc.: Pittsburgh, PA, 2004.
(26) Case, D. A.; et al. *Amber 9.0*; University of California: San Francisco, CA, 2002.
(27) Harris, J. G.; Yung, K. H. *J. Phys. Chem.* **1995**, *99*, 12021–12024.

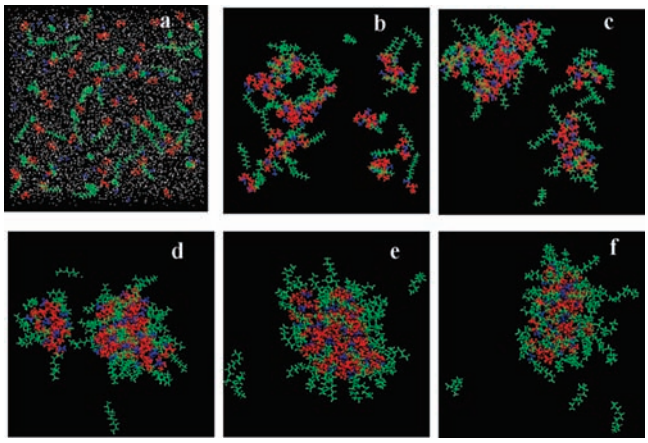

Figure 1. Time evolution of the ternary mixture of [TMG][Ac]/N-EtFOSA/CO_2 at $W_o = 0.8$. Snapshots are taken at (a) 0 ns (b) 0.3 ns (c) 5 ns (d) 30 ns (e) 100 ns and (f) 200 ns. Color scheme: red = cations; blue = anions; green = surfactants; white dots = C of CO_2. In (b−f), CO_2 is omitted for clarity.

molecular structures of each component along with their partial charges are included in Figure S1(Supporting Information).

Our first set of simulations with $W_o = 0.8$ was started from random mixtures of 48 ILs, 60 surfactants, and 6400 CO_2 molecules. These numbers correspond to [N-EtFOSA] = 0.06 g mL^{-1}, as was used in the experimental work of Han's group.[13] A large number of CO_2 molecules were included to generate a continuous CO_2 bulk phase. These simulations were carried out at 298 K and 20 MPa pressure, again the same experimental conditions as maintained by Han and co-workers. The second and third sets, corresponding to $W_o = 0.4$ and 1.2, were simulated, respectively, with 24 and 72 IL molecules at 10 and 38 MPa pressure. To enable the volume variation, simulations were performed in the NPT ensemble using the Nosé−Hoover thermostat and barostat. Both the thermostat and barostat relaxation times were set to 0.5 ps. Periodic boundary conditions were employed in all directions. The calculation of long-range Coulombic forces was performed by employing the full Ewald summation technique. The real space part of the Ewald sum and LJ interactions were cut off at 15 Å. SHAKE was used to constrain bond lengths between heavy atoms and hydrogens. A set of minimization and thermalization runs of the starting structures was performed to remove the initial bad contacts. All MD simulations were carried out for at least 100 ns. The minimizations and MD steps were performed by using the Amber 9.0 package.[26]

3. Results and Discussion

Figure 1 illustrates the spontaneous evolution of system 1 from a complete random distribution of the ternary mixture to an ordered aggregate of [TMG][Ac] that floats in continuous CO_2 phase. The appearance of a self-assembled inverted micelle consisting of IL core is in apparent agreement with the spectroscopic experiments of Han and co-workers.[13] The IL core is seen to be surrounded by surfactant headgroups, while the surfactant tails form a corona immersed in CO_2. The aggregation process takes place in succession, similar to that for water-in-CO_2 microemulsions. An initial faster clustering of polar components, [TMG][Ac] and N-EtFOSA headgroups, is followed by a slower fusion of the small aggregates to form three to six small reverse micelles (RM) of unequal sizes. This step follows a slow merging of the smaller micelles into two bigger

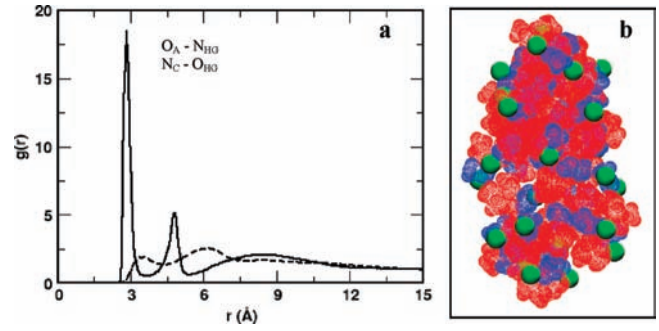

Figure 2. (a) Radial distribution functions for the [TMG][Ac]-surfactant pairs in system 1. Solid line: acetate-headgroups, dashed line: [TMG]-headgroups. The site−site distribution functions with maximum intensity in each category are compared. The respective pair of sites includes: O_{Ac}−N_{HG} and N_{TMG}−O_{HG}. (b) Time-averaged spatial density map of acetate anions (blue), [TMG] cations (red), and N-EtFOSA headgroups (green). The cations and anions are displayed in mesh representation and the headgroup center-of-masses are shown as beads.

micelles at around 30 ns. The single RM appears for the first time at 88 ns. This single aggregate remains stable thereafter although, on average, 3−6 surfactants dissociate and reassociate during the final 100 ns simulation run (panels e and f of Figure 1). Thus, direct evidence for the formation of IL droplets in the CO_2 phase emerges from this study.

At this juncture, the structural properties of the self-assembled droplet can be quantitatively compared to the available small-angle neutron scattering (SANS) data from a similar IL-in-oil microemulsion due to Eastoe et al.[21] The primary characteristics of a reverse micelle are the shape and size of its interior core. Similar to experimental findings, the simulation-generated droplet appears ellipsoidal in shape and measures nanometer in size. The radii of semi-minor (r) and semi-major axes (l) of the aggregate equal to 1.9 ± 0.3 nm and 3.4 ± 0.4 nm, respectively, with an aspect ratio (l/r) of 1.8. These values are in good agreement with the experimentally reported range of 1.9−2.4 nm for the semi-minor axis and 2.4−5.1 for the aspect ratio. The small deviation can be attributed due to the differential tail-solvent interactions. The area-per-headgroup, 140 ± 25 $Å^2$, also compares favorably with the experimentally measured value of 181 $Å^2$ for a similar perfluorooctyl sulfonamide surfactant.[28]

To learn more details about the structural properties of the reverse micelle, we consider various site−site radial distribution functions (rdf's). In Figure 2a, we plotted the rdf's for the anion−headgroup and cation−headgroup pairs in the [TMG][Ac]-based system. The anion−headgroup rdf shows a strong first coordination shell with a peak maximum at 2.8 Å and a distinct second peak at 4.8 Å. The rdf for cation−headgroup, on the other hand, shows two weak and broad peaks that appear at farther distances. The sharper and narrower peaks in the anion−headgroup pairs indicate that the acetate anions interact stronger with surfactant headgroups than the [TMG] cations. The time-averaged spatial density maps of IL cations, anions, and surfactant headgroups, as shown in Figure 2b, provide a direct evidence of such distribution. This figure clearly shows that the surfactant headgroups are largely populated around IL anions and favor stronger anion−headgroup interactions. This finding, however, contradicts the existing reports in literature, which hypothesize that the IL cation−surfactant H-bonding is responsible for the micellar stability.[13] Our results indicate that the H-bond formed

(28) Shrestha, R. G.; Shrestha, L. K.; Sharma, S. C.; Aramaki, K. *J. Phys. Chem. B* **2008**, *112*, 10520–10527.

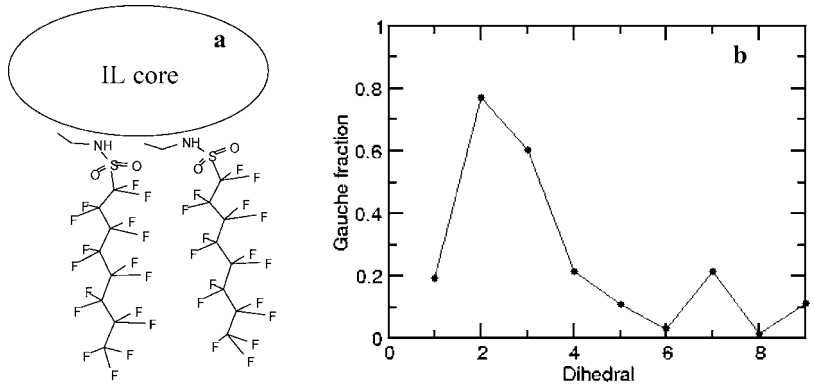

Figure 3. (a) Schematic diagram of the alignment of N-EtFOSA head and tails with respect to the [TMG][Ac] core. (b) Average fraction of gauche defects in each dihedral present along the backbone of the surfactant. The dihedral angles are numbered beginning with the $C_{CH3}-C_{CH2}-N-S$ fragment.

between the COO^- functional group of the IL acetate anions and the NH group of the surfactants is stronger than that between the NH_2^+ group of the [TMG] cation and the S═O group of the surfactants.

To support our finding, we provide a quantitative comparison of the interaction energies of IL anion−surfactants and IL cation−surfactants, average distances between the potential H-bond makers present in IL and surfactant moieties, and the probability of formation of such H-bonds. The respective values are given in Table 1. Even though both the energies fall in the typical H-bond energy range of 2−5 kcal/mol, the anion contribution is seen to be more significant always with a 100% probability of forming more stable H-bonds (quantified by shorter interatomic distances). Every analysis thus signifies that the stability of [TMG][Ac]/N-EtFOSA/CO_2 microemulsions mainly pertains to the anion−headgroup interactions, while the cations play a secondary role. The fact is, interheadgroup electrostatic repulsion is the weakest when bulky O═S═O groups allow the smaller NH groups to protrude inward to the IL core where the curvature is larger. A schematic diagram of the alignment of surfactant molecules relative to the IL core is depicted in Figure 3, along with the calculated gauche defects present in the surfactant tails.[29] Such a conformation leaves wider space for CO_2 to penetrate the tail region, thereby increasing the surfactant solubility—another major factor that contributes to microemulsion stability.[18,30]

A parallel simulation comprising the [BMIM][PF_6]/N-EtFOSA/CO_2 (system 2) also complements the experimental findings where a weaker IL core−surfactant interaction leads to a flickering aggregate under similar conditions. This is shown in Figure 4. A large portion of the [BMIM][PF_6] core is seen to be directly exposed to CO_2, and a large number of surfactant molecules are found to wander around at all times, indicating a weakly stable droplet. A quantitative measurement of the exposed core area can provide another metric to judge the stability of the systems. The calculated 44% exposed core area in system 2 was much larger than 17% in system 1.[31] Note that a large polar−apolar contact increases the surface tension and, hence, the free energy of the system, thereby destabilizing the microemulsion.[32]

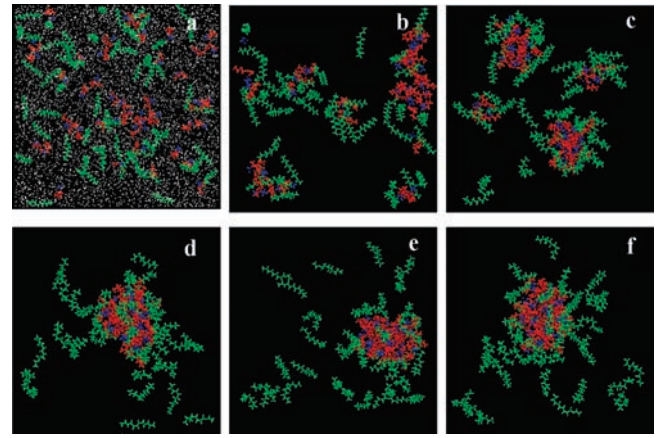

Figure 4. Time evolution of [BMIM][PF_6]/N-EtFOSA/CO_2 system. Snapshots are taken at (a) 0 ns, (b) 0.3 ns, (c) 3 ns, (d) 30 ns, (e) 50 ns, and (f) 100 ns. Color scheme: red = cations; blue = anions; green = surfactants; white dots = C of CO_2. In (b−f), CO_2 is omitted for clarity.

The weaker IL−surfactant interaction in [BMIM][PF_6] system is also reflected in rdf's and other statistical parameters. The peak intensities in Figure 5a imply that the anion, PF_6^- has a greater stabilizing influence than the $[BMIM]^+$ cation, and more importantly, the acetate ions in system 1 associate more strongly with the surfactant headgroups than the PF_6^- anions in system 2 (compare the peak heights in Figure 2a and Figure 5a). The reason is that the isotropic and bulkier PF_6^- cannot approach as close to the headgroup surface as the anisotropic CH_3COO^- groups could. The respective interaction energies, average H-bond distances, and the H-bond probabilities are included in Table 1. All these values compare much weaker than system 1 and explain why Liu et al.[13] could not get a stable microemulsion with [BMIM][PF_6] in their experiments.

To strengthen our finding further that the IL anions play the major role in microemulsion stability, we created two new systems by interchanging the anions in systems 1 and 2. As the rdf's in parts b and c of Figure 5 and the energetic and structural properties in Table 1 indicate, [BMIM][Ac] forms as stable a

(29) The angle is considered to be trans if it measures between 120−240°; the remainder is gauche.

(30) Lee, C. T., Jr.; Johnston, K. P.; Dai, H. J.; Cochran, H. D.; Melnichenko, Y. B.; Wignall, G. D. *J. Phys. Chem. B* **2001**, *105*, 3540–3548.

(31) The presence of small core exposure in reverse micelles was reported in the literature.[18] To quantify the exposure, first all CO_2 were removed from the system and a probe was rolled across the micellar surface. The accessible area due to IL cations and anions gives an estimate of the core exposure. To express this quantity in %, the area of the bare core was measured by removing all the surfactants from the droplet. A 2 Å probe that mimics CO_2 size was used.

(32) Lu, L.; Berkowitz, M. L. *J. Am. Chem. Soc.* **2004**, *126*, 10254–10255.

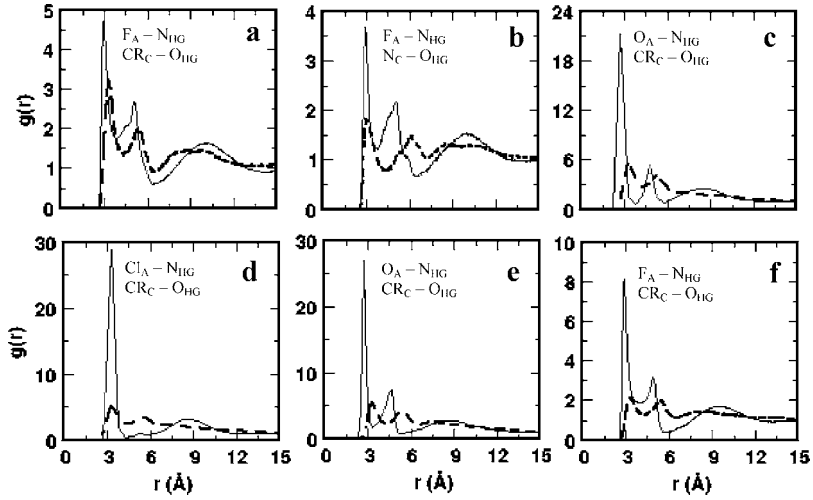

Figure 5. Site−site radial distribution functions for anion−headgroups (solid line) and cation−headgroups (dashed line) in (a) system 2, (b) system 3, (c) system 4, (d) system 5, (e) system 6, and (f) system 7. The respective pairs of sites are indicated in the graph. The shorter peak heights in the rdf's of systems 2, 3, and 7 are indicative of weaker IL−surfactant correlations.

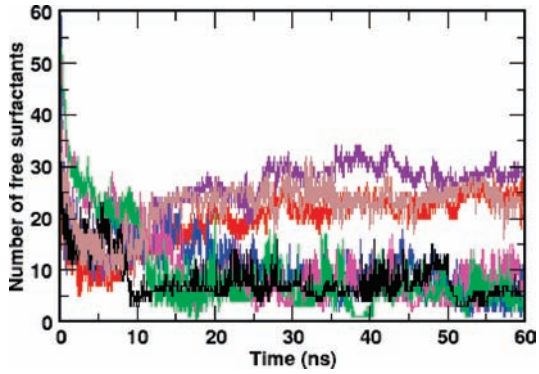

Figure 6. Comparative time evolution of the process of aggregation/deaggregation in systems 1−7. Color scheme: system 1 = black, system 2 = red, system 3 = violet, system 4 = blue, system 5 = magenta, system 6 = green, system 7 = brown. A large number of surfactants tends to dissociate from the surface of IL core in systems 2, 3, and 7, leaving huge polar−apolar contacts.

microemulsion as [TMG][Ac] did (compare the peak intensities of the rdf's in Figures 2a and 5c; and the E values of systems 1 and 4 in Table 1). In contrast, [TMG][PF_6]-based system 3 could not be stable (weak peak intensity in Figure 5b and small E values in Table 1, similar to the weakly stable system 2). We tested three more systems, 5−7 composed of common ILs. Results from Figure 5 and Table 1 again indicate that, irrespective of the nature of IL, the anions always interact more strongly with surfactants than the cations, as evident from larger anion−surfactant rdf peaks and greater E_{A-HG} values. Also, the strength of interactions primarily depends on the charge density on anions. Halogen-, acetate-, and nitrate-based ILs are likely to be more effective in stabilizing microemulsions in CO_2 than the PF_6- or BF_4-based ILs, as in the latter the anionic charges are more delocalized and hence interact less effectively with the surfactant headgroups. A comparative time evolution of aggregation/deaggregation of IL droplets in systems 1−7 is presented in Figure 6, by counting the free surfactants floating in solution over time. As Figure 6 indicates, the number of free surfactants started decreasing (from an initial value of 60) at the nucleation phase in all systems but exhibits a varied trend at longer times. Figure 6 clearly implies a greater stability of halogen-, acetate-, and nitrate-based IL systems (systems 1, 4, 5, and 6), where the surfactants remain associated with the IL core once they self-assemble. On the other hand, surfactants in PF_6- and BF_4-based systems (systems 2, 3, and 7) dissociate and reassociate constantly from the aggregate, leaving large polar−apolar contacts which subsequently can destabilize the microemulsion. The average number of free surfactants in later systems was as high as 30. Figure 6 is drawn up to 60 ns to observe the shorter time scale phenomenon (initial clustering during 0−12 ns) clearly.

We have also investigated the effect of W_o on the process of micellar self-assembly. The [TMG][Ac]-based system was reexamined at W_o = 0.4 and 1.2. A similar mechanism of aggregation, as in the system with W_o = 0.8, was seen to prevail. The faster clustering of polar components was followed by slower fusion of the small aggregates (Figures S2, S3 in Supporting Information). In both cases, the micellar shape was ellipsoidal. However, a large number of surfactants was seen to remain unassembled in the system with W_o = 0.4, even though the exposed area of the IL core was as low as 19%. This implies the existence of a stable droplet with an effective $W_o \approx 0.6$. As similar to the primary systems, the anion−headgroup pairs dominate the overall IL−surfactant interactions (Figure S4, Supporting Information), thereby greatly contributing toward the microemulsion stability.

4. Summary and Conclusions

Molecular dynamics simulations of random ternary mixtures of IL−fluorosurfactants−$scCO_2$ show the self-assembly of reverse micelles in supercritical carbon dioxide. The nanometer-sized, ellipsoidal-shaped ionic liquid droplets are found to be stabilized in the polar core of surfactant aggregates. This finding corroborates very well with the recent SANS and spectroscopic results. A more detailed analysis of the site−site radial distribution functions and the spatial density maps implies that the IL anions interact much more strongly with the surfactant headgroups than the IL cations. The energetic and hydrogen bond analyses show that the IL anions form stronger and more persistent H-bonds with the headgroup surface. Thus, we conclude that the stability of IL-in-CO_2 microemulsions mainly pertains to anion−surfactant interactions, while the IL cations play a secondary role. Our conclusions are supported by the fact that the miscibility of ILs with water and the solubility of

gases in ILs are mostly determined by associated IL anions.[33−39] The detailed knowledge derived here will aid in the judicious choice of IL anions and cations for obtaining the IL-in-CO_2 microemulsions with improved stability.

(33) Rivera-Rubero, S.; Baldelli, S. *J. Am. Chem. Soc.* **2004**, *126*, 11788–11789.
(34) Freire, M. G.; Santos, L. M. N. B. F.; Fernandes, A. M.; Coutinho, J. A. P.; Marrucho, I. M. *Fluid Phase Equilib.* **2007**, *261*, 449–454.
(35) Cammarata, L.; Peters, S. G.; Salter, P. A.; Welton, T. *Phys. Chem. Chem. Phys.* **2001**, *3*, 5192–5200.
(36) Anderson, J. L.; Dixon, J. K.; Brennecke, J. F. *Acc. Chem. Res.* **2007**, *40*, 1208–1216.
(37) Muldoon, M. J.; Aki, S. N. V. K.; Anderson, J. L.; Dixon, J. K.; Brennecke, J. F. *J. Phys. Chem. B* **2007**, *111*, 9001–9009.
(38) Anthony, J. L.; Anderson, J. L.; Maginn, E. J.; Brennecke, J. F. *J. Phys. Chem. B* **2005**, *109*, 6366–6374.
(39) Aki, S. N. V. K.; Mellein, B. R.; Saurer, E. M.; Brennecke, J. F. *J. Phys. Chem. B* **2004**, *108*, 20355–20365.

Acknowledgment. The financial support of the Department of Science and Technology (DST), and Department of Biotechnology (DBT), Government of India, is gratefully acknowledged.

Supporting Information Available: Force field parameters for the surfactants, ionic liquids, CO_2; validation of N-EtFOSA parameters; supporting Figures S1−S4; and complete references 25 and 26. This material is available free of charge via the Internet at http://pubs.acs.org.

JA1055005